IEEE Access
Multidisciplinary | Rapid Review | Open Access Journal

Received May 22, 2019, accepted June 11, 2019, date of publication June 19, 2019, date of current version July 3, 2019.

Digital Object Identifier 10.1109/ACCESS.2019.2923817

Evaluation and Transformation of Unrealizable Tasks for Robot Systems in Representation Space

JIANBO SU, (Senior Member, IEEE)
Research Center of Intelligent Robotics, Shanghai Jiao Tong University, Shanghai 200240, China
e-mail: jbsu@sjtu.edu.cn

This work was supported in part by the key project of the National Natural Science Foundation of China under Grant 61533012 and Grant 91748120.

ABSTRACT This paper proposes a framework for a robot system to actively evaluate its realizability for a specific task based on its representation space. The representation space (R-space) of a robot system could be constructed to describe the distributions of system attributes (called representation), whose transitions reflect the process of task realization. All factors blocking transitions of the system representation, hence the task realization, including physical configurations of the robot system and environmental constraints, are defined as unreachable areas in the R-space, specifying the limitation of the system's capability to execute the prescribed task. The reachable area in the R-space, showing the representations that the robot system could be of, is figured out to formalize the criteria for task realizability. The potential optimal scheme to accomplish a realizable task can further be recognized from the shortest path that the robot representation transits along. Otherwise, causes for unrealizable tasks are investigated to suggest clues for transforming the tasks to be realizable ones. Meanwhile, conditions and the total cost to fix unrealizable tasks are compared to make out the best strategy under the given cost index, if there is more than one scheme. The proposed framework is applied to the typical task of path planning for a robot manipulator and parking task of a mobile robot to show its effectiveness as well as its performance.

INDEX TERMS Task realizability, representation space, robot manipulator, mobile robot.

I. INTRODUCTION

One of the constructive goals of robotics is to enable a robot to actively and autonomously achieve various tasks without frequent human intervention [1]. Most of the robot systems are generally designed for specific applications, such as industrial productions, environmental monitoring or entertainment, etc..When a robot is allocated a specific task, it implies that the task is realizable by the robot available with particular configurations of sensor and actuation. Limited by internal configurations and external constraints, any robots are not so universal in its capability that they can only accomplish a set of specified tasks. With increasingly complex tasks and variable environments, it is getting more and more difficult to describe all factors that may affect task realization process for a robot. This means a robot may frequently not be able to realize a prescribed task with limited sensing and actuation, and/or due to dynamic and unpredictable environmental dynamics. Hence, it is more practical and efficient to evaluate if a robot of specific configurations could complete an assigned task prior to task planning. Furthermore, it is also desirable to see if an unrealizable task to the available robot could be transformed to be a realizable one by adjusting any conditions with acceptable costs.

Robot manipulator, as the most traditional type of robot system, has accumulated the widest range of applications since 1960s [2]. Limited translations or rotations could only be executed by the manipulator with limited number of joints in its limited range of degree-of-freedoms. This is so-called physical constraints of a robot manipulator system. On the other hand, constraints in robotic physical space, no matter static or dynamic, may prevents the manipulator from moving freely [3]. Generally, path planning of a robot system is either realized in the affiliated configuration space [4]–[6] or workspace [7]–[10]. The concept of configuration enables investigations of different motion planning task by differently configured robots in a unified framework, while the workspace is described as the set of all possible actions the robot can realize [11]. There have been much work on

The associate editor coordinating the review of this manuscript and approving it for publication was Yingxiang Liu.

evaluating the feasibility of robot motion planning based on workspace [12]–[14]. A feasible motion planning exists for a robot manipulator only if the planned trajectory lies entirely in its workspace [12]. The feasibility analysis was conducted by evaluations of a set of algebraic equations supposing the workspace description is simple enough geometrically. However, this scheme becomes inapplicable if joint limits of a robot system are taken into account.

For most wheeled mobile robots (WMRs), the kinematic constraints are nonholonomic, which impose huge difficulty in controlling and analyzing the whole system [15], [16]. Taking account of inertia and power limits of actuators, as well as obstacles in physical space, the movability of WMRs is constrained to a great extent. Yamamoto *et al.* propose a real-time optimization method based on receding horizon control which satisfies nonholonomic kinematic constraints for WMRs [17]. Kahoul *et al* propose a stochastic trajectory planning method considering static obstacles in [18]. Nevertheless, these methods are only applicable when the parking tasks are realizable. Moreover, research on path planning of a manipulator and motion planning of a WMR have separately been conducted with different schemes, which imposes essential difficulties on coordinations of operation manipulator and mobile agent due to lack of a unified framework.

R-space-based method has been proposed to deal with the evaluations of the realizability for a prescribed task before it is truly executed [19]–[21]. Efficiency in recognizing optimal realization procedures is also validated for different tasks [22], [23]. However, more emphasis is located on recognizing optimal schemes for realizable tasks instead of fixing unrealizable tasks. This issue is to be deeply investigated in this paper. Framework on transforming an unrealizable task into a realizable one is discussed based on R-space. A general procedure of identifying causes for unrealizable tasks is first discussed to provide technical implications to transform unrealizable tasks into realizable ones. Critical factors and costs of transforming unrealizable tasks can be reached to work out the most energy-efficient strategy.

The remainder of this paper is organized as follows. Realizability by a robot system of specific configurations to a prescribed task is discussed in Section II in the framework of the R-space. Applications on trajectory planning of a robot manipulator and parking task of a mobile robot are respectively demonstrated in Sections III and IV to show the capacity of R-space, followed by Conclusions in Section V.

II. TASK REALIZABILITY BASED ON R-SPACE

When accomplishing any task, physical representations and attributes of a robot system involved in task execution varies continuously from the beginning of the task to the end. Meanwhile, environmental presences may also be changed due to the robotic manipulations to realize the task, which accumulatively reflect the realization procedure of the specific task. Practically, R-space could be constructed with reduced dimensions by physical attributes of the system coupled with the robot representations and the task realizations, including positions and poses of the robot systems as well as factors featuring environment. More task-relevant capabilities of the robot systems, including repeatability, accuracy, and sensing modalities, etc. could be formulated possibly by involving more irrelevant R-spaces. The procedure of a task realization could thus be transformed to a process of the system representation transition in its affiliated R-space.

A. CRITERIA FOR REALIZABLE TASKS

If there are m variables describing the task realization by a robot of specific configurations, a m dimensional representation space can be constructed as:

$$X = (x_1, x_2, \ldots, x_m), \tag{1}$$

where $x_i (i = 1, 2, \ldots, m)$ are configurations or Cartesian parameters and $x_{imin} \leq x_i \leq x_{imax}$. The start and goal representations of the robot for the task executed could be specified by:

$$\begin{cases} X^S = (x_1^S, x_2^S, \ldots, x_m^S), \\ X^G = (x_1^G, x_2^G, \ldots, x_m^G). \end{cases} \tag{2}$$

Generally speaking, there are three kinds of system constraints: physical constraints, obstacle constraints and task constraints. Physical constraints stand for mechanical restrictions such as limitations of joint motions. Obstacle constraints are from working environment, caused by obstacles in physical space which may block robots' movement. Most often, a particular task could also impose constraints on robot motion planning, such as energy or time consumed, which are referred as task constraints. These constraints could be depicted as the unreachable areas in the R-space, which is denoted as R_{obs}. The remaining areas in R-space, denoted as R_{free}, describes the reachable areas for system representations during the process of task executions. An example of a 2-D R-space is shown in Fig.1. A task is evaluated to be realizable if both the start representation X^S and the goal one X^G are locating inside the reachable area of the R-space. Meanwhile, a path P connecting X^S and X^G exists inside R_{free}, denoting transitions of the representation of the robot to conduct the particular task:

$$\begin{cases} X^S, & X^G \in R_{free}, \\ \exists P \subset R_{free}, & P = \{X^S, \ldots, X^i, \ldots, X^G\}. \end{cases} \tag{3}$$

where X^i is one of a series of mid-points located in the representation transit trajectory from X^S to X^G.

B. FACTORS FIGURING FOR UNREALIZABLE TASKS

A task is unaccomplishable if either condition in (3) is destroyed. Under this condition, factors that affect the realizability of the prescribed task should hence recognized. More importantly, strategies may further be recognized and evaluated by finding possible solutions for (3) with acceptable costs to transform an unrealizable task to a realizable one.

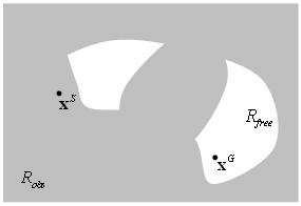

FIGURE 1. An example of the R-space.

It is straightforward to remove constraints one by one until a realization strategy can eventually be located.

From Fig.1, we can see that there is no path in R_{free} connecting X^S and X^G since the starting representation X^S lies in R_{obs}. When the obstacle constraints are removed, the updated R-space is shown in Fig.2. The location of X^S changes to be in the reachable area. However, X^S and X^G are still not connectable. The R-space of the robot to conduct the task is updated and shown in Fig. 3 after removing both obstacle and physical constraints. It is easy to see that the initial and goal representations can now be connected. Therefore, it can be seen that the unrealizability of the task is caused by both the obstacle and the physical constraints.

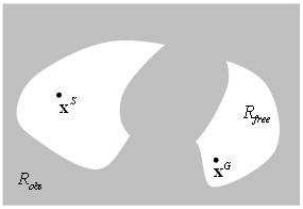

FIGURE 2. The updated R-space after obstacle constraints removed.

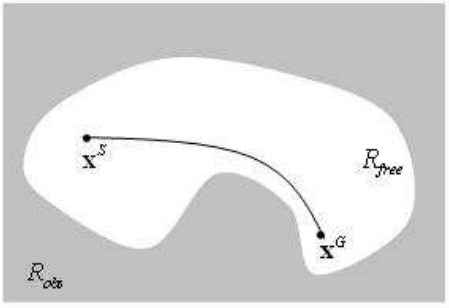

FIGURE 3. The updated R-space after both obstacle and physical constraints removed.

C. REALIZABILITY TRANSFORMATION OF THE UNREALIZABLE TASKS

Inherent reasons for a task to be unrealizable by a robot of specific configurations are gradually recognized by step-by-step removing constraints in its affiliated R-space. However, this is not a general solution to fix unrealizable tasks. Practically, it might be more convincible to release any constraints with new degrees-of-freedom. Task realizability of a reconfigured robot to execute a newly-defined task could thus be explored in the updated R-space with the new dimension x_{new}:

$$\xi = (x_1, x_2, \ldots, x_m, x_{new}). \tag{4}$$

The corresponding starting and goal representations are ξ^S and ξ^G, respectively.

$$\begin{cases} \xi^S = (x_1^S, x_2^S, \ldots, x_m^S, x_{new}^S), \\ \xi^G = (x_1^G, x_2^G, \ldots, x_m^G, x_{new}^G). \end{cases} \tag{5}$$

The R-space is grided with a set of discretized parameters [21], [22] and the optimal path between ξ^S and ξ^G is searched by A* algorithm in the discretized R-space [24]. Here is an example for the cost function of A*:

$$f(n) = g(n) + h(n), \tag{6}$$

where

$$\begin{cases} g(n) = \sum_{i=0}^{n-1} \sqrt{\sum_{j=1}^{m} (x_j^i - x_j^{i+1})^2 + (x_{new}^i - x_{new}^{i+1})^2}, \\ h(n) = \sqrt{\sum_{j=1}^{m} (x_j^n - x_j^G)^2 + (x_{new}^n - x_{new}^G)^2}. \end{cases} \tag{7}$$

In (7), $g(n)$ represents the cost from the starting node to the node n and $h(n)$ is the cost from the node n to the final one.

Note that there are certainly different kinds of motion freedoms for a robot system to impose, reflecting different strategies to transfer an unrealizable task to be a realizable one.

III. PATH PLANNING OF A ROBOT MANIPULATOR

A. MANIPULATOR KINEMATICS

R-space is first used to explore the realizability of a 2-link robot manipulator (shown in Fig.4) executing different tasks. L_1 and L_2 are respectively the lengths of link 1 and link 2. θ_1 and θ_2 are respectively the rotation angles of two joints. Given joint angles θ_1 and θ_2, coordinates of the end-effector (x, y) can completely be described by the forward kinematics:

$$\begin{bmatrix} x \\ y \end{bmatrix} = \begin{bmatrix} L_1 \cos\theta_1 \\ L_1 \sin\theta_1 \end{bmatrix} + \begin{bmatrix} L_2 \cos(\theta_1 + \theta_2) \\ L_2 \sin(\theta_1 + \theta_2) \end{bmatrix}. \tag{8}$$

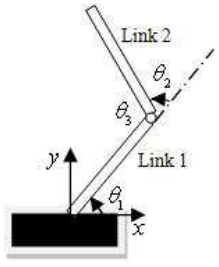

FIGURE 4. A robot manipulator with two revolute links.

B. R-SPACE

The position and orientation of a 2-link manipulator can be defined by its joint angles (θ_1, θ_2). Therefore, dimensions of the R-space of the robot manipulator in Fig.4 can thus be specified as

$$q = (\theta_1, \theta_2). \tag{9}$$

Note that the R-space can be updated if the degrees-of-freedom of the manipulator is re-configured. For instance, if the base of the manipulator is moveable, degrees-of-freedom describing the motions of the base should be added as new dimensions in the updated R-space. Normally, once the robot manipulator is re-configured, the R-space should be updated to include all representations critical to the realizations of the given task. From the task realization point of view, capability of a robot manipulator and factors from its surroundings can be viewed as a whole. Therefore, dimensions for describing the environment information can also be included in the affiliated R-space when needed.

C. SINGLE OBSTACLE

The proposed R-space framework is employed to find a feasible path for a robot manipulator to avoid a ball obstacle when moving in its workspace. The task is transformed to be realizable first by trial and test scheme, and then by re-construction of the affiliated R-space.

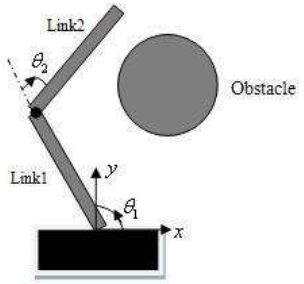

FIGURE 5. The manipulator and its physical space.

The robot system and its surroundings are shown in Fig.5. Lengths of 2 links are $L_1 = L_2 = 0.5m$, and rotation ranges of two joints are $0 \le \theta_1 \le \pi, 0 \le \theta_2 < 2\pi$. A ball obstacle is centered at (0.3, 0.6)with radius $0.2m$. The start and goal configurations of the manipulator, (θ_1, θ_2), are $S(120°, 30°)$ and $G(15°, 30°)$, respectively. Its corresponding R-space could then be described by Eq. (9). Hence, the starting and goal representations are respectively written as $q^S = (120°, 30°)$ and $q^G = (15°, 30°)$. Sampling intervals of θ_1 and θ_2 are respectively $I_1 = 1°$ and $I_2 = 2°$. The affiliated R-space is gridded in R^2 with the predefined sampling intervals. Each cell is labeled as reachable or unreachable one by computing whether the cell leads to collision with the obstacle, as shown in Fig.6, in which black area is unreachable for the system representation. Obviously, the starting and goal representations q^S and q^G both lie in reachable areas. However, no

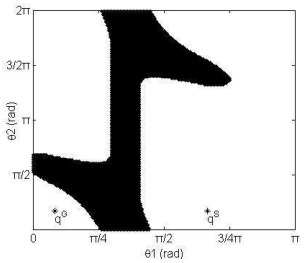

FIGURE 6. The R-space when the obstacle is centered at (0.3, 0.6).

connecting path could be found between q^S and q^G. Hence, this task is unrealizable by the robot of this configuration.

Since the black area is formed from the obstacle, it is intuitive to first move the spatial position of the obstacle to change the realizability of the task. When the obstacle shifts from (0.3, 0.6) to (0.5, 0.6), the updated R-space is shown in Fig.7, showing that the reachable areas in the updated R-space is enlarged with this scheme. But the task remains unrealizable since no connecting path can be found from q^S and q^G.

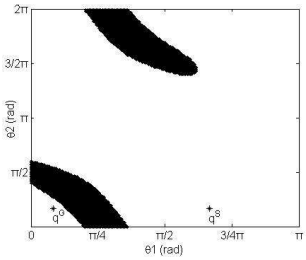

FIGURE 7. The R-space when the obstacle is centered at (0.5, 0.6).

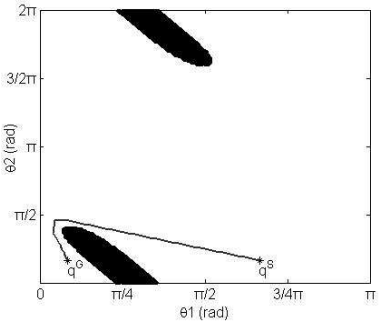

FIGURE 8. R-space when the obstacle is centered at (0.6, 0.8).

When the obstacle is moved to the position of (0.6, 0.8), Fig.8 shows the affilated R-space. A path could now be found connecting the start and goal representations, which means that the task is realizable. Furthermore, the optimal scheme is possibly obtained for the representation of the robot to transfer in it R-space, by, e.g., minimizing the length of the

representation corresponding to task realization (Fig. 8):

$$J = \sum_{i=0}^{n-1} \sqrt{(\theta_1^i - \theta_1^{i+1})^2 + (\theta_2^i - \theta_2^{i+1})^2}, \quad (10)$$

where n is the number of points along the optimal path for representation variations. In this case, the optimal trajectory for the end-effector is of the following cost:

$$J_1 = \sum_{i=0}^{31} \sqrt{(\theta_1^i - \theta_1^{i+1})^2 + (\theta_2^i - \theta_2^{i+1})^2} = 143.25. \quad (11)$$

which corresponds to the task realization procedure shown in Fig.9.

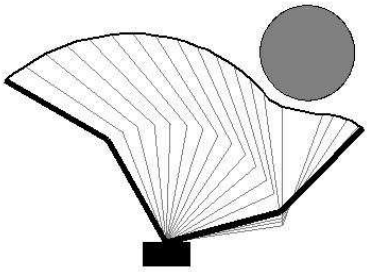

FIGURE 9. The trajectories of joints and end-effector in physical space.

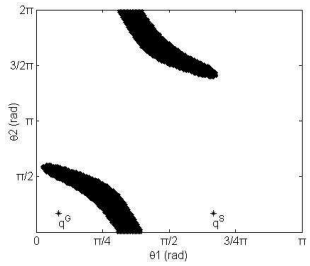

FIGURE 10. R-space when the obstacle is with radius 0.1.

Alternatively, the task could also be changed its realizability by shrinking the obstacle's size. The resultant R-space for the robot system to conduct the task is shown in Fig.10 after the size of the ball is changed from radius $0.2m$ to $0.1m$. No connecting path could be found due to the safe distance considered in the path searching. But it also shows that the reachable areas is enlarged (the unreachable areas are reduced) compared with that of Fig. 6 and Fig. 7, which means this kind of strategy is effective to fitness of task realization. When the radius of the ball further shrinks to 0.06, the optimal path could be obtained, see Fig.11. The corresponding trajectories for the position change of the end-effector and joint angle variations to realize the task are shown in Fig.12. The total cost of the optimal path is computed:

$$J_2 = \sum_{i=0}^{53} \sqrt{(\theta_1^i - \theta_1^{i+1})^2 + (\theta_2^i - \theta_2^{i+1})^2} = 162.91. \quad (12)$$

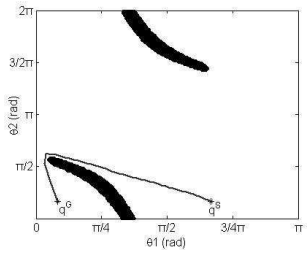

FIGURE 11. R-space when the obstacle is with radius 0.06.

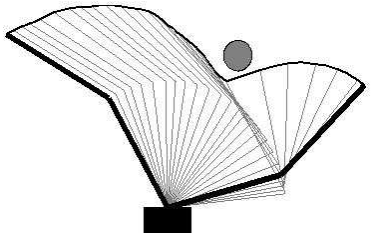

FIGURE 12. The trajectories of joints and end-effector in physical space.

Comparing Eq. 11 and Eq. 12, we can see that $J_1 < J_2$. This means the first strategy is better than the second one under the given cost index. However, since we use the trial and test scheme to fix the realizability of a task, it is not straightforward to recognize clues to transform the task successfully. Specifically, it is still not clear how to relocate the obstacle to change a specific extent of task realizability. This issue could further be investigated by integrating the obstacle distribution in the R-space.

Firstly, the ball obstacle is assumed to be relocated along the horizontal axis. Suppose $c_x \in [-1.2, 1.2]$, where c_x stands for the x coordinate of the obstacle center. The R-space with the new dimension (parameter) can be written as:

$$\xi = (\theta_1, \theta_2, c_x). \quad (13)$$

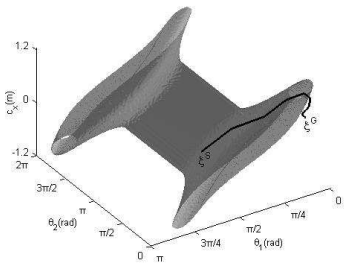

FIGURE 13. R-space with added parameter c_x.

The start and goal representations are respectively $\xi^S = (120°, 30°, 0.3)$ and $\xi^G = (15°, 30°, 0.3)$. The R-space is shown in Fig.13, in which the optimal path connecting ξ^S and ξ^G is found. Thus, the minimum range of c_x can be obtained from the optimal path. In this case, $c_x \in [0.3, 1.08]$. Since moving the obstacle is energy consuming, the cost function

takes the following forms:

$$\begin{cases} J_3 = \sum_{i=0}^{53} C_i = 152.04, \\ C_i = \sqrt{(\theta_1^i - \theta_1^{i+1})^2 + (\theta_2^i - \theta_2^{i+1})^2 + (c_x^i - c_x^{i+1})^2}. \end{cases} \tag{14}$$

Secondly, the obstacle is assumed to move along the vertical axis. Similarly, range of the y coordinate of the obstacle center is set as $c_y \in [-1.2, 1.2]$. The R-space is:

$$\eta = (\theta_1, \theta_2, c_y). \tag{15}$$

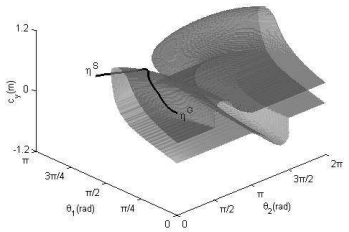

FIGURE 14. R-space with added parameter c_y.

The starting representation is $\eta^S = (120°, 30°, 0.6)$ and the goal one is $\eta^G = (15°, 30°, 0.6)$. Fig.14 shows the optimal representation variations for task realization in the system and task affiliated R-space. The optimal range of c_y is [0.6, 1.14]. The cost is calculated as follows:

$$\begin{cases} J_4 = \sum_{i=0}^{43} C_i = 123.53, \\ C_i = \sqrt{(\theta_1^i - \theta_1^{i+1})^2 + (\theta_2^i - \theta_2^{i+1})^2 + (c_y^i - c_y^{i+1})^2}. \end{cases} \tag{16}$$

Here, the position of the obstacle ball has been incorporated in the affiliated R-space as a new dimension and an extended parameter defining the realizability of the specific task. Transformation of a task from unrealizable to realizable one has successfully been conducted. To figure out the optimal, eg., the most energy-efficient strategy, to fulfill the task, two more strategies are proposed on the condition that the manipulator base is movable. Suppose the manipulator is able to move along the horizontal axis. The corresponding R-space is updated with an additional dimension b_x, which represents the x coordinate of the manipulator base. We have $b_x \in [-1, 1]$ initially. The R-space is denoted as:

$$\zeta = (\theta_1, \theta_2, b_x). \tag{17}$$

The starting and goal representations are $\zeta^S = (120°, 30°, 0)$ and $\zeta^G = (15°, 30°, 0)$, respectively. Trajectory planning for system representation is shown in Fig.15. The feasible range of b_x for the task to be realizable is $[-0.82, 0]$. The cost could be computed by:

$$\begin{cases} J_5 = \sum_{i=0}^{54} C_i = 156.23, \\ C_i = \sqrt{(\theta_1^i - \theta_1^{i+1})^2 + (\theta_2^i - \theta_2^{i+1})^2 + (b_x^i - b_x^{i+1})^2}. \end{cases} \tag{18}$$

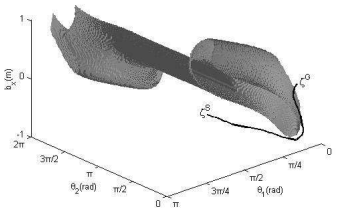

FIGURE 15. R-space with added parameter b_x.

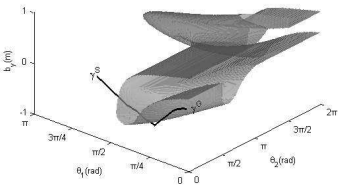

FIGURE 16. R-space with added parameter b_y.

Similarly, the R-space could be re-written as follows if the manipulator is enable to move along the vertical axis:

$$\gamma = (\theta_1, \theta_2, b_y), \tag{19}$$

where $b_y \in [-1, 1]$. The start and goal representations are respectively $\gamma^S = (120°, 30°, 0)$ and $\gamma^G = (15°, 30°, 0)$. Fig.16 shows the trajectory planning for system representation for this task. To fix the task, the critical condition is $b_y \in [-0.58, 0]$. The cost is calculated as:

$$\begin{cases} J_6 = \sum_{i=0}^{44} C_i = 125.42, \\ C_i = \sqrt{(\theta_1^i - \theta_1^{i+1})^2 + (\theta_2^i - \theta_2^{i+1})^2 + (b_y^i - b_y^{i+1})^2}. \end{cases} \tag{20}$$

By comparing costs of different strategies denoted in (14),(16),(18) and (20), we have $J_4 < J_6 < J_3 < J_5$. On one hand, it is more energy-efficient to fix the task through relocating the obstacle than the manipulator base. On the other hand, fixing the task by adjusting the obstacle location or the manipulator base in the vertical direction outweighs those of the horizontal direction.

D. MULTIPLE OBSTACLES

Realizability of a path planning task in cluttered environment is of more interest in practice. For a given task, different obstacles may affect the task feasibility variously. In order to fix an unrealizable task, it is necessary to identify which obstacle prevents the task from being accomplished.

The manipulator and its physical space is shown in Fig.17. The length of each link is $0.5m$, and the coordinates of the manipulator base is $(1, 1)$. Two circular obstacles are scattered in the environment. One obstacle with radius of $0.2m$ is centered at $(1.3, 1.66)$, and the other with radius $0.15m$ is centered at $(0.7, 1.4)$. Scopes for robot joint angles are $0 \le \theta_1 \le \pi$ and $0 \le \theta_2 < 2\pi$, respectively. The manipulator is assigned with three path planning tasks shown in Table 1.

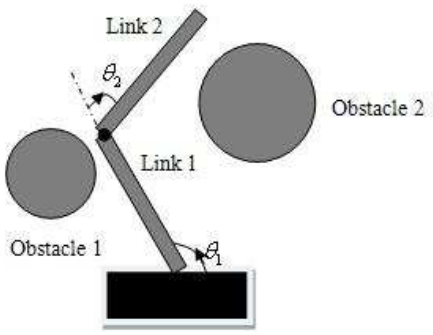

FIGURE 17. The manipulator and two obstacles in physical space.

TABLE 1. The initial and final configurations of three path planning tasks.

	Start	Goal
Task 1	$S_1(30°, 30°)$	$G_1(90°, 30°)$
Task 2	$S_2(90°, 180°)$	$G_2(170°, 90°)$
Task 3	$S_3(15°, 60°)$	$G_3(170°, 100°)$

1) TASK 1

The R-space is constructed with joint angles θ_1 and θ_2, the same as (11). The initial and final representations of the robot system for Task 1 are $q^{S_1} = (30°, 30°)$ and $q^{G_1} = (90°, 30°)$, respectively. It is easy to see in Fig. 18 that there is no connecting path between q^{S_1} and q^{S_2}. In order to figure out which obstacle prevents the Task from being completed, we consider two obstacles separately. Fig.19 shows the R-space when only Obstacle 1 is considered (Similarly, it is easy to obtain the R-space when only considering Obstacle 2). Therefore, we can see that Task 1 is unrealizable due to Obstacle 2. According to the previous discussions, Task 1 might be fixed by relocating Obstacle 2 or augmenting movability of the manipulator base. For convenience, we list the results in Table 2. The R-space is built with added parameter c_{2x}, c_{2y}, b_x and b_y, where c_{2x} and c_{2y} are respectively the x and y coordinates of Obstacle 2, and b_x and b_y are those of the manipulator base. It is easy to see from Table 2 that fixing Task 1 by relocating Obstacle 2 in the vertical axis (c_{2y} involved) or augmenting movability of the manipulator base in the vertical direction (b_y involved) are equally the most energy-efficient.

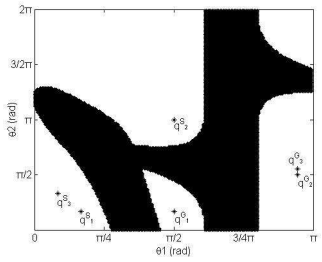

FIGURE 18. The R-space considering both obstacles.

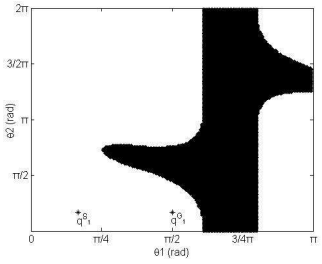

FIGURE 19. The R-space when only obstacle 1 is considered.

2) TASK 2

Similarly, Task 2 is diagnosed as unrealizable because no path can be found between $q^{S_2} = (90°, 180°)$ and $q^{G_2} = (170°, 90°)$, which are respectively the initial and final representations of the robot system for Task 2. Obviously, Task 2 is unrealizable due to the presence of the Obstacle 1. Task 2 is fixed by relocating Obstacle 1 or augmenting movability of the manipulator. Evaluations of the two transferring schemes are shown in Table 3. It is easy to see that relocating Obstacle 1 (c_{1y} involved) or augmenting the movability of the manipulator base in the vertical axis (b_y involved) outweigh the other two strategies.

3) TASK 3

Fig.18 shows that $q^{S_3} = (15°, 60°)$ and $q^{G_3} = (170°, 100°)$, which are the initial and final representations of the robot system for Task 3, cannot be connected in the R-space. It also implies that Task 3 is unrealizable due to both obstacles. Fig.20 is the R-space after augmenting movability of the manipulator base in the horizontal axis. The critical condition is that $b_x \in [1, 1.74]$. Correspondent cost of fixing Task 3 in this scheme is 191.07. On the other hand, Fig.21 is the R-space when the manipulator base is augmented it movability in the vertical axis. The critical condition is $b_y \in [0.54, 1]$ and the total cost is 171.14. Obviously, augmenting movability of the manipulator base in the vertical axis is more energy-efficient than that of the horizontal axis.

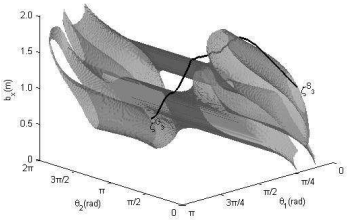

FIGURE 20. The R-space after augmenting movability in horizontal axis.

It is easy to see that the proposed R-space based strategy for task realizability evaluation does not rely on the number of the degrees-of-freedom (DOFs) of the robot manipulator. Constructions and dimensions of the affiliated R-space for a robot manipulator only relates to the impacts relevant to conduct a prescribed task, including internal and external factors. In this sense, it might be of similar complexities for

TABLE 2. Comparison among different strategies for fixing Task 1.

R-space	Initial representation	Final representation	Critical condition	Cost
$\xi = (\theta_1, \theta_2, c_{2x})$	$\xi^{S_1} = (30°, 30°, 1.3)$	$\xi^{G_1} = (90°, 30°, 1.3)$	$c_{2x} \in [1.3, 2.06]$	122
$\eta = (\theta_1, \theta_2, c_{2y})$	$\eta^{S_1} = (30°, 30°, 1.66)$	$\eta^{G_1} = (90°, 30°, 1.66)$	$c_{2y} \in [1.66, 2.16]$	83.36
$\zeta = (\theta_1, \theta_2, b_x)$	$\zeta^{S_1} = (30°, 30°, 1)$	$\zeta^{G_1} = (90°, 30°, 1)$	$b_x \in [0.28, 1]$	133.27
$\gamma = (\theta_1, \theta_2, b_y)$	$\gamma^{S_1} = (30°, 30°, 1)$	$\gamma^{G_1} = (90°, 30°, 1)$	$b_y \in [0.5, 1]$	83.36

TABLE 3. Comparison among different strategies for fixing Task 2.

R-space	Initial representation	Final representation	Critical condition	Cost
$\xi = (\theta_1, \theta_2, c_{1x})$	$\xi^{S_2} = (90°, 180°, 0.7)$	$\xi^{G_2} = (170°, 90°, 0.7)$	$c_{1x} \in [0.42, 0.7]$	98.57
$\eta = (\theta_1, \theta_2, c_{1y})$	$\eta^{S_2} = (90°, 180°, 1.4)$	$\eta^{G_2} = (170°, 90°, 1.4)$	$c_{1y} \in [1.4, 1.64]$	96.73
$\zeta = (\theta_1, \theta_2, b_x)$	$\zeta^{S_2} = (90°, 180°, 1)$	$\zeta^{G_2} = (170°, 90°, 1)$	$b_x \in [1, 1.28]$	98.57
$\gamma = (\theta_1, \theta_2, b_y)$	$\gamma^{S_2} = (90°, 180°, 1)$	$\gamma^{G_2} = (170°, 90°, 1)$	$b_y \in [0.76, 1]$	96.73

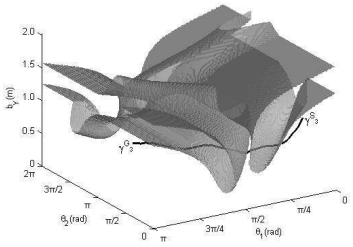

FIGURE 21. The R-space after augmenting movability in vertical axis.

affiliating the R-space of a 2-DOF robot manipulator with that of a 6 DOFs manipulator, so long as they are prescribed the same task in the same environment.

IV. PARKING PROBLEM OF A WHEELED MOBILE ROBOT

A. SYSTEM KINEMATICS

As shown in Fig.22, the main part of the Wheeled Mobile Robot (WMR) is a rigid chassis with motorized wheels. There is no slipping between the wheels and the chassis. Moreover, the WMR cannot move sidelong. (x, y) denotes the coordinates of the robot center. θ is the angle between the horizontal axis and the direction of robot movement. v and ω are respectively the linear and angular speeds of the robot.

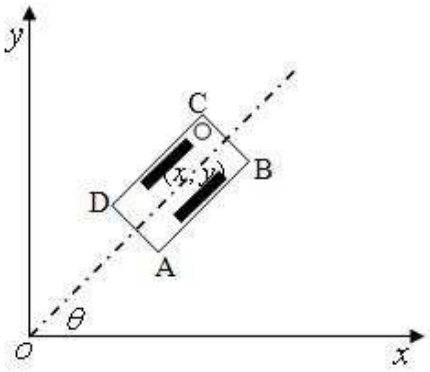

FIGURE 22. The model of the WMR.

The simplified kinematics can be written as:

$$\begin{cases} \dot{x} = v \cdot \cos\theta \\ \dot{y} = v \cdot \sin\theta. \\ \dot{\theta} = \omega \end{cases} \tag{21}$$

B. THE R-SPACE

Three different parking tasks are considered, moving from S to G_1, G_2 and G_3, respectively, see Fig.23. As shown in Fig.22, (x, y, θ) specifies the position and orientation of the WMR, which is defined as the configuration of the robot. The WMR is required to move from an initial configuration to a final configuration. Thus, the R-space of the robot can be defined as

$$\zeta = (x, y, \theta). \tag{22}$$

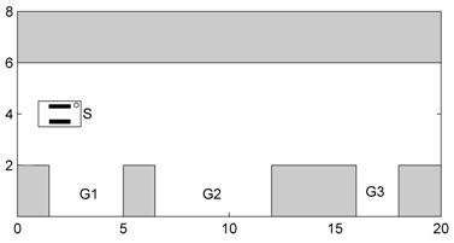

FIGURE 23. Three parking tasks in physical space.

Subject to various types of constraints, the WMR presents limited capability in task realization which can be analyzed by means of R-space. Reachable area of R-space, which is composed of all the representations the system can be of, provides insights into the robot's ability to accomplish tasks. Hence, unreachable area reflects influences that all the constraints have upon the robot's capability of task realization. The ranges of x, y, θ values are $0 \le x \le 20m$, $0 \le y \le 8m$, $-90° \le \theta \le 90°$, respectively.

C. OPTIMAL STRATEGIES TO REALIZABLE TASKS

Three parking problems are considered for the WMR to show evaluations of the task realizability in its R-space.

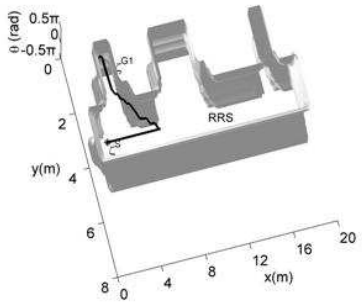

FIGURE 24. Path of Task 1 in the R-space.

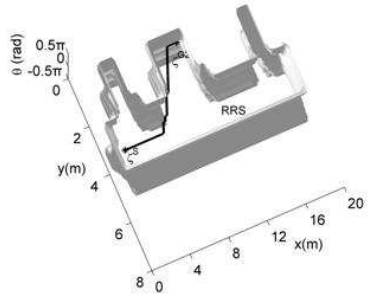

FIGURE 25. Path of Task 2 in the R-space.

TABLE 4. The initial and final representations of the WMR for three parking tasks.

	$\zeta^S = (x^S, y^S, \theta^S)$	$\zeta^G = (x^G, y^G, \theta^G)$
Task 1	$(2, 4, 0)$	$(3, 1, 0)$
Task 2	$(2, 4, 0)$	$(10.6, 1, 0)$
Task 3	$(2, 4, 0)$	$(17, 1.2, 0)$

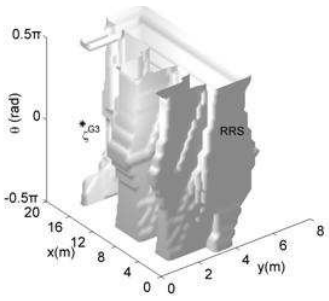

FIGURE 26. The goal representation of Task 3 is out of the reachable area.

The initial and final representations of the WMR are listed in Table 4. Their correspondent R-spaces are constructed as before, shown in Figs 24, 25, and 26. For Task 1 and Task 2, the start and goal representations of the WMR are both within the reachable area of R-space. Fig.24 shows that a connected trajectory within the reachable area for Task 1. Similarly, Fig.25 presents the connected trajectory for Task 2.

D. SOLUTION TO UNREALIZABLE TASK

As shown in Fig.26, the goal representation of Task 3 is not within the reachable area of the R-space. Herein, we fix the task by substituting the unreachable goal representation with, e.g., its nearest neighbor representation, i.e., $\zeta^{G_4} = (17, 1.2, 90°)$, within the reachable area in its RS. This scheme is intuitively much cheaper than endowing the mobile robot with such as jumping or flying function. Fig.27 shows that a connected path between ζ^S and ζ^{G_4} is found. It is for sure that the task is finally realized with most possibly condensed performance.

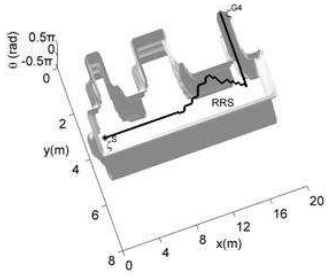

FIGURE 27. Path of Task 3 in the R-space.

V. CONCLUSION

This paper has proposed a framework to evaluate task realizability based on the affiliated R-space. Consequently, the optimal strategy of task accomplishment could be recognized for a robot systems of specific configurations. Given a robot system with a predefined task, the affiliated R-space is constructed, in which the reachable and unreachable areas defined respectively by internal and external constraints are located, which implies system's ability to accomplish the task. Criteria for evaluating the realizability of a robot system to a specific task are proposed. Scheme for task realization is converted to recognition of the path transition in R-space for its representations. Guidance will be provided to fix unrealizable task, with consequently optimal strategy for realizable task be further derived. The proposed strategy has been verified through tasks on path planning of a robot manipulator and parking of a mobile robot. For the manipulator, path planning tasks under a single obstacle and cluttered environments are evaluated. Three parking problems of the WMR are solved using the proposed framework.

Future work includes investigating task realizability with more task-relevant capabilities of the robot systems, including repeatability, accuracy, and sensing modalities, etc.. More systematic way could be explored denoting efficient or even the optimal strategies to change task realizability of a robot system in its affiliated R-space. Besides, considering dynamic constraints is also a tough issue when evaluating task realizability of any robot systems. Furthermore, recognizing and allocating the robot of best efficiency among a group of robots to accomplish a given task is surely of more interest.

REFERENCES

[1] J. C. Latombe, *Robot Motion Planning*. Norwell, MA, USA: Kluwer, 1998.

[2] L. Sciavicco and B. Siciliano, *Modelling and Control of Robot Manipulators*. London, U.K.: Springer-Verlag, 1996.

[3] J. Su, "Robotic task realizability in representation space," in *Proc. IEEE Int. Conf. Syst., Man, Cybern.*, Oct. 2015, pp. 2766–2771.

[4] T. Lozano-Perez, "A simple motion-planning algorithm for general robot manipulators," *IEEE J. Robot. Automat.*, vol. 3, no. 3, pp. 224–238, Jun. 1987.

[5] K. Chen, Y. Zhang, J. Yi, and T. Liu, "An integrated physical-learning model of physical human-robot interactions with application to pose estimation in bikebot riding," *Int. J. Robot. Res.*, vol. 35, no. 12, pp. 1459–1476, 2016.

[6] Z. Jiang, Z. Dou, W. X. Zhao, J.-Y. Nie, M. Yue, and J.-R. Wen, "Supervised search result diversification via subtopic attention," *IEEE Trans. Knowl. Data Eng.*, vol. 30, no. 10, pp. 1971–1984, Oct. 2018.

[7] O. Khatib, "A unified approach for motion and force control of robot manipulators: The operational space formulation," *IEEE J. Robot. Autom.*, vol. 3, no. 1, pp. 43–53, Feb. 1987.

[8] J.-H. Shin and J.-J. Lee, "Dynamic control of underactuated manipulators with free-swinging passive joints in Cartesian space," in *Proc. IEEE Int. Conf. Robot. Automat.*, vol. 4, Apr. 1997, pp. 3294–3299.

[9] X. Xu and Y. Chen, "A method for trajectory planning of robot manipulators in Cartesian space," in *Proc. World Congr. Intell. Control Automat.*, vol. 2, Jun./Jul. 2000, pp. 1220–1225.

[10] G. Antonelli, S. Chiaverini, M. Palladino, G. P. Gerio, and G. Renga, "Cartesian space motion planning for robots. An industrial implementation," in *Proc. Int. Workshop Robot Motion Control*, Jun. 2004, pp. 279–284.

[11] B. Roth, "Performance evaluation of manipulators from a kinematic viewpoint," in *Performance Evaluation of Programmable Robots and Manipulators*. New York, NY, USA: NBC Special Publication, 1975, pp. 39–61.

[12] H. Zhang, "Efficient evaluation of the feasibility of robot displacement trajectories," *IEEE Trans. Syst., Man, Cybern.*, vol. 23, no. 1, pp. 324–330, Jan. 1993.

[13] X. Yang, B. Wang, K. Yang, C. Liu, and B. Zheng, "A novel representation and compression for queries on trajectories in road networks," *IEEE Trans. Knowl. Data Eng.*, vol. 30, no. 4, pp. 613–629, Apr. 2018.

[14] Y. S. Guan, H. Zhang, X. Zhang, and Z. Guan, "Workspace generation for multifingered manipulation," *Adv. Robot.*, vol. 25, no. 18, pp. 2293–2317, 2011.

[15] F. Belkhouche, "Nonholonomic robots navigation using linear navigation functions," in *Proc. Amer. Control Conf.*, Jul. 2007, pp. 5328–5332.

[16] Y. Tian, J. Das, and N. Sarkar, "Near-optimal autonomous pursuit evasion for nonholonomic wheeled mobile robot subject to wheel slip," in *Proc. IEEE Int. Conf. Robot. Autom.*, May 2010, pp. 4946–4951.

[17] M. Yamamoto, M. Iwamura, and A. Mohri, "Quasi-time-optimal motion planning of mobile platforms in the presence of obstacles," in *Proc. IEEE Int. Conf. Robot. Autom.*, May 1999, pp. 2958–2963.

[18] L. Kahoul and A. E. Lehtihet, "A random profile approach to minimum-time parking problems for non-holonomic wheeled mobile robots," *J. Autom. Syst. Eng.*, vol. 1, no. 1, pp. 22–31, 2007.

[19] W. Xie and J. Su, "Trajectory planning for robot manipulators based on state space," in *Proc. 7th World Congr. Intell. Control Automat.*, Jun. 2008, pp. 4831–4836.

[20] W. L. Xie and J. B. Su, "A new coordination method for multi-robot system," *High Technol. Lett.*, vol. 15, no. 1, pp. 1–6, 2009.

[21] J. Su and W. Xie, "Motion planning and coordination for robot systems based on representation space," *IEEE Trans. Syst., Man, Cybern. Syst.*, vol. 41, no. 1, pp. 248–259, Feb. 2011.

[22] A. L. Jennings and R. Ordóñez, "Unbounded motion optimization by developmental learning," *IEEE Trans. Cybern.*, vol. 43, no. 4, pp. 1178–1188, Aug. 2013.

[23] Z. Zhang and Y. Zhang, "Acceleration-level cyclic-motion generation of constrained redundant robots tracking different paths," *IEEE Trans. Syst., Man, Cybern. B, Cybern.*, vol. 42, no. 4, pp. 1257–1269, Aug. 2012.

[24] S. Tang, Y. Zhang, Z.-X. Xu, H.-J. Li, Y.-T. Zheng, and J.-T. Li, "An efficient concept detection system via sparse ensemble learning," *Neurocomputing*, vol. 169, no. 2, pp. 124–133, Dec. 2015.

JIANBO SU (SM'04) received the B.S. degree in automatic control from Shanghai Jiao Tong University, Shanghai, China, in 1989, the M.S. degree in pattern recognition and intelligent systems from the Institute of Automation, Chinese Academy of Science, Beijing, China, in 1992, and the Ph.D. degree in control science and engineering from Southeast University, Nanjing, China, in 1995.

He joined the faculty of the Department of Automation, Shanghai Jiao Tong University, Shanghai, in 1997, where he has been a Full Professor, since 2000. His current research interests include robotics, pattern recognition, and human–machine interaction. He has published three books and over 270 peer-reviewed technical papers, and holds over 20 patents in these areas. He is a member of the Technical Committees of Networked Robots and Human–Machine Interactions, and a Standing Committee Member of the Chinese Association of Automation. He received the Best Associate Editor Award from the IEEE SMC Society, in 2014. He is currently serving as an Associate Editor for the IEEE TRANSACTIONS ON CYBERNETICS, the *International Journal of Social Robotics*, and the *International Journal of Humanoid Robotics and Control Theory and Applications*.